A novel 40-Gb/s all-optical inverted wavelength converter based on a modified terahertz optical asymmetric demultiplexer

Xuetian Huang (黄学田), Peida Ye (叶培大), Min Zhang (张 民), and Ling Wang (王 凌)

Optical Communication Center, Beijing University of Posts & Telecommunications, Beijing 100876

Received June 18, 2004

A novel scheme for all-optical inverted wavelength conversion with 40-Gb/s pseudorandom bit sequences (PRBSs) based on a modified terahertz optical asymmetric demultiplexer (TOAD) is proposed. The performance of the proposed wavelength converter is analyzed in term of extinction ratio (ER) through numerical simulations. For a typical ER of 10 dB, some key characteristic parameters of the semiconductor optical amplifier (SOA) are designed. With the properly designed parameters, a high quality eye diagram is achievable, indicating that the amplitude fluctuation of the output signal is effectively reduced.

OCIS codes: 250.5980, 060.2330, 060.0060.

All-optical wavelength converter has been considered to be one of the key devices in future wavelength-division-multiplexed (WDM) networks, since it allows reuse of wavelengths, avoids wavelength channel contention, and thus provides for more flexible and novel network management[1−3]. Up to now, most integrated wavelength converters use the Mach-Zehnder (M-Z) interferometer, which requires two semiconductor optical amplifiers (SOAs), hence balancing the interferometer becomes a hard task. The terahertz optical asymmetric demultiplexer (TOAD), on the other hand, uses a single SOA and the clockwise and the counter clockwise signals traverse the same optical path, thereby negating the effects of optical path length difference. Monolithically integrated TOADs are thus used for all-optical wavelength conversion, but it can only work with 10-Gb/s full duty cycle signals[4]. In this letter, a novel all-optical wavelength converter based on a modified TOAD is proposed, where wavelength conversion can be implemented with 40-Gb/s pseudorandom bit sequences (PRBSs).

The modified TOAD is composed of an optical loop mirror, a SOA placed asymmetrically, and an intraloop 3-dB polarization preserving coupler, as shown in Fig. 1. The probe pulse enters the interferometer at port 1 and splits into two counter-propagating pulses of the same amplitude and identical phase: a clockwise (CW) pulse and a counter-clockwise (CCW) pulse. Because of the position asymmetry Δx, the CW pulse, and the CCW pulse arrive at the SOA at different times with a delay of $\delta\tau$ ($\delta\tau = 2\Delta x/n_{\rm g}$, where $n_{\rm g}$ is the group speed of the lightwave in the fiber loop). The data signal and an additional periodic signal with the repetition rate corresponding to the bit rate are both injected into the SOA via a multiplexer acting as control signals. The data pulse is timed to arrive at the SOA $\delta\tau$ ahead of the periodic pulse. Furthermore, the CW pulse is timed to arrive at the SOA after the data pulse with a time lag of $\delta\tau/2$ and the CCW pulse is timed to arrive at the SOA after the periodic pulse. When a logical "1" is present in the data signal, i.e., the periodic signal and the data signal are identical, the CW pulse and the CCW pulse will experience approximately equal gain and identical phase shift and then interfere destructively in the intraloop coupler. Therefore, the output of the interferometer is "0". On the other hand, with a "0" in the data signal, the two counterpropagating pulses will experience different gains and phase shifts, resulting in a pulse at the output.

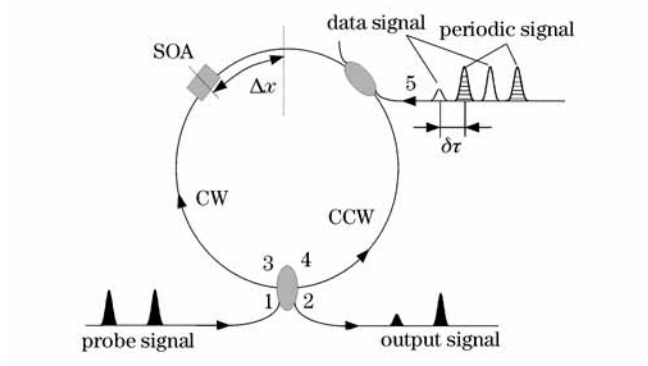

Fig. 1. Schematic diagram of the proposed wavelength converter.

In our simulations, the intensity of the control-signal lights is assumed to be much larger than that of the probe light, so that the dynamic gain of the SOA is only controlled by the control-signal lights. The two counterpropagating probe pulses only probe the change of refractive index of the SOA caused by the intense control pulses. Moreover, the control pulses induced nonlinearities in the other parts of the modified TOAD are assumed to be negligible.

Since the control-pulse energy is 200 fJ in this letter, the SOA can be treated with a simplified model given by J. M. Tang, which does not include the effects of two-photon absorption (TPA) and ultrafast nonlinear refraction (UNR), as follows[5]

$$\frac{\partial g(z,t)}{\partial t} = \frac{g_0 - g(z,t)}{\tau_{\rm C}} - \frac{g(z,t)}{1+\varepsilon P_C(z,t)}\frac{P_{\rm C}(z,t)}{E_{\rm sat}}, \quad (1)$$

$$\frac{\partial P_{\rm C}(z,t)}{\partial z} = \frac{[g(z,t)-\alpha_{\rm int}]}{1+\varepsilon P_{\rm C}(z,t)} P_{\rm C}(z,t), \quad (2)$$

$$\frac{\partial \phi_{\rm C}(z,t)}{\partial z} = -\frac{1}{2}\alpha \frac{g(z,t)}{1+\varepsilon P_{\rm C}(z,t)}, \quad (3)$$

where $P_{\rm C}(z,t)$ and $\phi_{\rm C}(z,t)$ are the power and the phase-shift of the control signals, respectively. $g(z,t)$ is the dynamic gain coefficient of the SOA, g_0 is the small-signal gain, $\tau_{\rm C}$ is the spontaneous carrier lifetime, α is the linewidth enhancement factor, $\alpha_{\rm int}$ is the internal loss, ε is the nonlinear gain compression factor due to intraband processes, such as carrier heating and spectral hole-burning, and $E_{\rm sat}$ is the saturation energy, which satisfies

$$E_{\rm sat} = P_{\rm sat} \cdot \tau_{\rm C}, \tag{4}$$

where $P_{\rm sat}$ is the saturation power of the SOA.

Amplified spontaneous emission (ASE) noise from the wavelength converter is assumed to be negligible since the SOA is nearly always strongly saturated by the high power levels of both the data and periodic signals. In addition, the signal independent Gaussian noise and the internal loss of the SOA are neglected for simplicity. Then, the transmittance of the modified TOAD can be expressed as

$$T(t) = \frac{1}{4}\{G_{\rm CW}(t-\delta\tau) + G_{\rm CCW}(t) - 2\sqrt{G_{\rm CW}(t-\delta\tau)G_{\rm CCW}(t)} \times \cos[\Delta\Phi_{\rm CW}(t-\delta\tau) - \Delta\Phi_{\rm CCW}(t)]\}, \tag{5}$$

where $G_{\rm CW}(t)$, $\Delta\phi_{\rm CW}(t)$, $G_{\rm CCW}(t)$, and $\Delta\phi_{\rm CCW}(t)$ are the power dynamic gain and nonlinear phase shift experienced by the two counter-propagating probe pulses, thus the wavelength-converted inverted signal power emerging from port 2 can be obtained as

$$P(t) = P_{\rm PRB}(t)T(t), \tag{6}$$

where $P_{\rm PRB}(t)$ is the power of the probe pulses.

In the numerical simulations, the data signal used is a 40-Gb/s RZ PRBS with a word length of 2^7-1. The data pulses and the periodic pulses are assumed to have the same wavelength, intensity, and polarization. The other default modeling parameters of the SOA and the characteristics of the data pulses and the probe pulses are listed in Table 1. Using the method given by Refs. [6,7], the dynamic gain of the SOA can be calculated. Furthermore, the extinction ratio (ER), which can evaluate the opening of the eye diagram, is utilized to optimize the performance of the wavelength converter.

A portion of the simulation results with the input bit sequences being "10011010" is shown in Fig. 2. The data signal is illustrated in Fig. 2(a), and the periodic signal is also given with the dot line. It is observed in Fig. 2(b) that the SOA is nearly always strongly saturated by the periodic signal and the data signal. The SOA gain ranges from 4.70 to 7.79 dB. The influence of the previous pulse on the present pulse is thus mitigated. The dependence of the SOA gain on the data signal becomes weak in the presence of the periodic signal. However, the data signal imparts a phase change to the probe pulses, which saves the bit information. In the absence of the data pulse, the SOA gain has more time to recover. The relative large gain difference between the CW and the CCW pulses imparts a phase change of about $\pi/2$ rad, resulting a pulse at the port 2, as shown in Figs. 2(c) and (d). In the presence of the data pulse, however, the corresponding phase change is approximately 0. Therefore the output is also "0".

Table 1. Default Parameters

Description	Value
Nonlinear Gain Compression Factor (ε) (W^{-1})	0.3
Linewidth Enhancement Factor (α)	4
Refractive Index of SOA ($n_{\rm SOA}$)	3.62
Light Velocity (c) (m/s)	3.0×10^8
Wavelength of Data Signal ($\lambda_{\rm s}$) (nm)	1530
Wavelength of Probe Signal ($\lambda_{\rm P}$) (nm)	1550
Pulse-Width of Data Pulses ($T_{\rm CT}$) (ps)	4
Pulse-Width of Probe Pulses ($T_{\rm P}$) (ps)	4
Energy of Data Pulses ($E_{\rm C}$) (fJ)	200
Energy of Probe Pulses ($E_{\rm R}$) (fJ)	10
Data Signal Extinction Ratio ($ER_{\rm D}$) (dB)	30
Time Asymmetry of the Modified TOAD ($\delta\tau$) (ps)	12.5

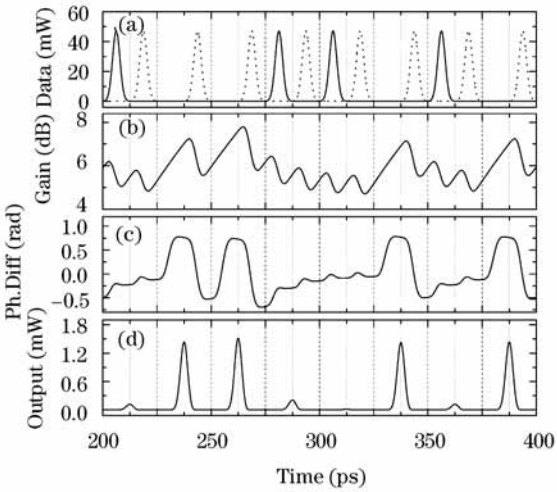

Fig. 2. A portion of the simulation results with the input bit sequences being "10011010". The input data (a), the dynamic gain (b), the phase difference between the CW and CCW pulses when the meet in the intraloop coupler (c), and the output signal (d) are all shown when $\tau_{\rm C}$ = 100 ps, $P_{\rm sat}$= 10 dB, $L_{\rm SOA}$= 100 μm, g_0 = 20 dB.

Figure 3 shows the ER of the output signal as a function of the SOA length under different SOA carrier lifetimes (70, 100, and 150 ps). It is noted that when the SOA is shorter than 250 μm, the ER fluctuates slightly with increasing the SOA length, namely, the influence of the SOA length on the ER can be neglected when it is less than 250 μm. However, when the SOA is longer than 250 μm, the ER falls sharply. It is also noted that a small carrier lifetime is favorable to get a large ER. For a carrier lifetime of 100 ps, the ER fluctuates with an average of about 11.1 dB. In this sense, to obtain a specific ER (typically 10 dB in practice), SOA carrier lifetime and length should be less than 100 ps and 250 μm, respectively.

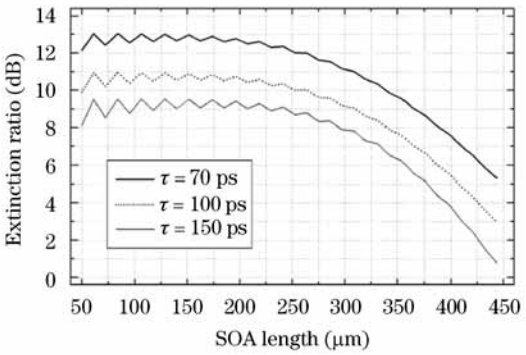

Fig. 3. ER versus SOA length under different SOA carrier lifetimes (70, 100, 150 ps). g_0= 20 dB, $P_{\rm sat}$ = 10 dBm.

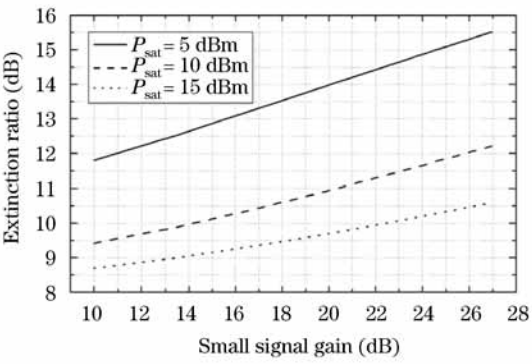

Fig. 4. ER versus small signal gain under different saturation powers (5, 10, 15 dBm). g_0= 20 dB, $\tau_{\rm C}$ = 100 ps, $L_{\rm SOA}$ = 100 μm.

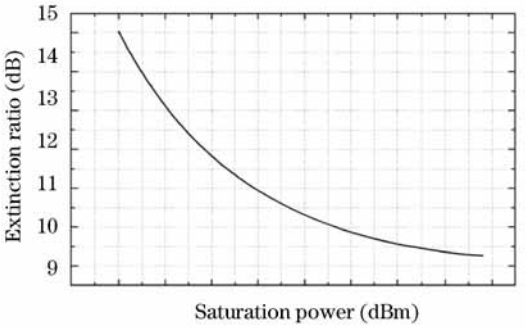

Fig. 5. ER versus small signal gain. g_0= 20 dB, $L_{\rm SOA}$= 100 μm, $\tau_{\rm C}$ = 100 ps.

The impacts of the small signal gain on the ER of the output signal under different saturation powers (5, 10, and 15 dBm) are shown in Fig. 4. It is observed that the ER increases linearly with the increase of the small signal gain. When the small signal gain is 20 dB, the ER is about 11.1 dB, which is consistent with Fig. 3. It is also noted in Fig. 4 that a small saturation power is favorable to get a large ER, which is also demonstrated in Fig. 5.

Figure 6 is the eye diagram of the wavelength-converted signal when $\tau_{\rm C}$ = 100 ps, $P_{\rm sat}$= 10 dBm, g_0= 20 dB, and

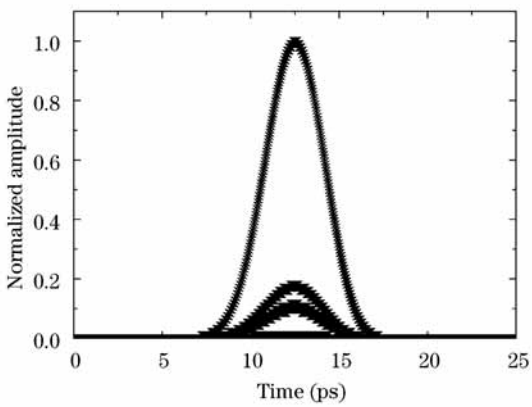

Fig. 6. Eye diagram of the wavelength-converted signal when $\tau_{\rm C}$ = 100 ps, $P_{\rm sat}$= 10 dB, $L_{\rm SOA}$= 100 μm, g_0 = 20 dB.

$L_{\rm SOA}$= 100 μm. Obviously, the upper and the lower amplitudes of "1" are almost equal, which indicates that the amplitude fluctuation of the "1" level is effectively suppressed. The amplitude of "0" varies. Nevertheless, the lower amplitude of "1" is still about 7.47 dB larger than the upper amplitude of "0".

Proposed in this letter is a novel scheme for 40-Gb/s all-optical wavelength conversion based on a modified TOAD. The feasibility of wavelength conversion with the proposed scheme is demonstrated through numerical simulations. Meanwhile, some restrictions are placed on the key characteristic parameters of the SOA. Simulation results indicate that a high quality output signal with a larger than 10-dB ER is achievable. A high quality eye diagram is also achievable, indicating that the amplitude fluctuation of the output signal is effectively reduced.

This work was supported by the National "863" Project of China (No. 2003AA122530) and the National Natural Science Foundation of China (No. 60372100). X. Huang's e-mail address is sameoul@hotmail.com.

References

1. M. Asghari, I. H. White, and R. V. Penty, J. Lightwave Technol. **15,** 1181 (1997).
2. S. L. Danielsen, P. B. Hansen, K. E. Stubkjaer, M. Schilling, K. Wunstel, W. Idler, P. Doussiere, and F. Pommerau, IEEE Photon. Technol. Lett. **10,** 60 (1998).
3. T. Durhuus, B. Mikkelsen, C. Joergensen, S. L. Danielsen, and K. E. Studkjaer, J. Lightwave Technol. **14,** 942 (1996).
4. V. M. Menon, W. Tong, C. Q. Li, F. Xia, I. Glesk, P. R. Prucnal, and S. R. Forrest, in *Proceedings of the 15th Annual Meeting of the LEOS* 49 (2002).
5. J. M. Tang, P. S. Spencer, and K. A. Shore, J. Lightwave Technol. **16,** 86 (1998).
6. C. Xie and P. Ye, Chin. J. Lasers (in Chinese) **27,** 525 (2000).
7. Y. Zhang and P. Ye, Acta Opt. Sin. (in Chinese) **22,** 99 (2002).